Journal of Electrotechnology, Electrical Engineering and Management (2025)
Clausius Scientific Press, Canada
DOI: 10.23977/jeeem.2025.080112
ISSN 2560-6697 Vol. 8 Num. 1

Based on CIE1931 Multi-Channel Color Conversion and Point-by-Point Calibration Optimization Method for LED Displays

Wen Li[1,*], Shaolong Liu[1], Xinyu Miao[2], Tiansheng Sun[1]

[1]*School of Electrical Engineering, Yingkou Institute of Technology, Yingkou, Liaoning, 115000, China*
[2]*Yingkou Abe Wiring Co., Ltd., Yingkou, Liaoning, 115000, China*
[*]*Corresponding author*

Keywords: LED Display; Color Space Conversion; Color Gamut Mapping; Multi-Channel Display

Abstract: With the development of display technology, the demand for high-fidelity color reproduction in LED displays has become increasingly prominent. Aiming at the problems of color gamut mismatch between video sources and display devices, complexity of multi-channel signal conversion, and chromaticity non-uniformity of pixels, this study constructs a systematic optimization scheme based on the CIE1931 color space. First, a color gamut mapping model from BT2020 to sRGB is designed, achieving minimum perceptual error under gamut compression through optimization of the color difference function. Second, for the conversion requirement from four channels to five channels, a multi-primary color mapping method integrating linear transformation and residual compensation is proposed to enhance color gamut expression capability using the new channels. Additionally, a point-by-point calibration algorithm based on local response function inversion is developed to solve the problem of pixel display non-uniformity. Test results show that the proposed method significantly improves color reproduction accuracy and display uniformity, providing theoretical and technical support for the design and optimization of high-performance LED displays.

1. Introduction

In recent years, with the rapid development of display technology, the application of LED displays in advertising media, stage performances, public information display, and other fields has experienced explosive growth. High-fidelity color reproduction has become the core driving force for promoting the iteration of display technology [1]. Modern colorimetry uses the CIE1931 standard color space as the theoretical foundation to construct a mathematical framework for cross-device color measurement and conversion. However, in engineering practice, the color gamut mismatch between video sources and display devices, the dimensional complexity of multi-channel signal conversion, and the chromaticity non-uniformity of LED pixel arrays still constitute key technical bottlenecks restricting the improvement of display quality [2].

Technically, the color gamut space defined by high-definition video standards such as BT2020 significantly exceeds the color expression range of ordinary RGB displays, inevitably causing perceptual errors during color conversion [3]. The differences in the number of primary colors and spectral response characteristics between the four-channel RGBV video source and the five-channel RGBCX display system make multi-primary color mapping face the problems of dimensional expansion and color difference balance (as shown in Figure 1) [4]. The non-uniformity of semiconductor manufacturing processes causes LED pixels to exhibit significant chromaticity dispersion under uniform input excitation, seriously affecting the visual consistency of display images [5].

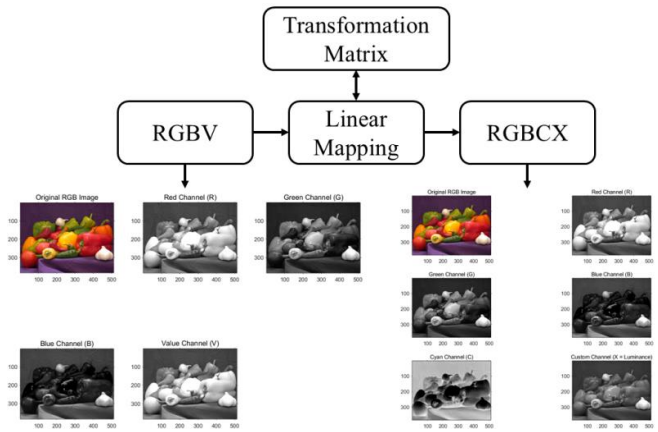

Figure 1: Schematic diagram of multi-channel linear mapping process

Existing studies show that traditional color space conversion methods mostly rely on linear mapping models, which are difficult to balance the human visual perception characteristics described by the CIEDE2000 color difference model and the nonlinear constraints of color gamut boundaries [6]. Point-by-point calibration technologies generally lack adaptability to multi-channel display systems and struggle to achieve high-precision color reproduction in extended gamut scenarios [7]. How to minimize color conversion errors and maximize display uniformity under existing hardware conditions through mathematical modeling and algorithm optimization has become an important issue to be urgently addressed in the current display field.

Based on the above background, this study builds an optimization system covering "color gamut mapping-multi-channel conversion-point-by-point calibration" based on the CIE1931 color space theory [8]: optimizes the color gamut mapping from BT2020 to sRGB by constructing a loss function based on perceptual color difference, proposes a multi-primary color mapping method integrating linear transformation and residual compensation to solve the dimensional conversion problem from RGBV to RGBCX [9], and develops a point-by-point calibration algorithm based on local response function inversion to improve the display uniformity of pixel arrays [10], providing a technical solution with both theoretical depth and practical value for the engineering design of high-performance LED display systems.

2. Optimization of Color Gamut Mapping from BT2020 to sRGB

The color gamut space defined by the BT2020 high-definition standard covers a significantly larger area in the CIE1931 chromaticity diagram than ordinary RGB displays. Measured data show that the geometric area of the BT2020 color gamut is 0.211866, while the target sRGB color gamut area is only 0.112050, resulting in approximately 47.11% of colors being unable to be directly reproduced. This type of conversion is essentially a projection problem from a high-dimensional color gamut to a low-dimensional space, requiring balancing geometric mapping accuracy and

human visual perception characteristics during gamut compression. In the space standardization link, the RGB values input by BT2020 are mapped to the CIEXYZ tristimulus value space through a transformation matrix, which is defined as shown in Equation (1):

$$M_{\mathrm{BT}\to\mathrm{XYZ}} = \begin{bmatrix} 0.6369 & 0.1446 & 0.1689 \\ 0.2627 & 0.6780 & 0.0593 \\ 0.0000 & 0.0281 & 1.0610 \end{bmatrix} \tag{1}$$

This matrix is calibrated through standard spectral response data to achieve linear transformation from the BT2020 color space to XYZ. In the chromaticity normalization step, normalized chromaticity values are obtained through coordinate transformation as shown in Equation (2):

$$x = \frac{X}{X+Y+Z}, y = \frac{Y}{X+Y+Z} \tag{2}$$

This step projects three-dimensional color information onto a two-dimensional chromaticity plane to facilitate subsequent color gamut boundary determination. For chromaticity points beyond the sRGB color gamut, a projection strategy based on CIEDE2000 is adopted to achieve optimal fitting by minimizing perceptual color difference. The optimization process constructs a loss function with the CIEDE2000 color difference model as the core to quantify the perceptual difference between the source color and the mapped color in the Lab space, subject to dual constraints: first, ensuring that the DE error of key colors (such as white and three primary colors) is controlled within the visually acceptable range (typically DE<5), and second, ensuring that the mapped RGB values are within the [0,1] physical driving interval. Through this framework, the conversion coverage rate from the BT2020 color gamut to sRGB is finally achieved at 52.89%, providing a basis for high-fidelity color reproduction of LED displays. The model constructs a loss function with the CIEDE2000 color difference formula as the core to quantify the perceptual difference between the source color and the mapped color in the Lab space, with a specific form as shown in Equation (3):

$$\mathcal{L}_{\mathrm{color}} = E_{00}(L^*_{\mathrm{src}}, a^*_{\mathrm{src}}, b^*_{\mathrm{src}}, L^*_{\mathrm{map}}, a^*_{\mathrm{map}}, b^*_{\mathrm{map}}) \tag{3}$$

Where the Lab coordinates are obtained through the nonlinear transformation of XYZ values. This model fits human visual characteristics through weighting factors and is suitable for high-fidelity display scenarios. For colors beyond the sRGB color gamut, a "linear fitting + saturation compression" strategy is adopted: first, generate candidate RGB values through a linear function, then process the out-of-gamut part, and finally minimize $\mathscr{L}_{\mathrm{colour}}$ through iterative optimization. The transformation matrix $\mathrm{M}_{\mathrm{BT2020}\to\mathrm{RGB}}$ is solved by least squares fitting, with a specific form as shown in Equation (4):

$$\mathrm{M}_{\mathrm{BT2020}\to\mathrm{RGB}} = \begin{bmatrix} 1.34406118 & -0.18430056 & -0.26121879 \\ -0.33907319 & 1.19501007 & -0.10069263 \\ -0.00498799 & -0.01070950 & 1.36191141 \end{bmatrix} \tag{4}$$

This matrix improves mapping accuracy through a nonlinear compensation mechanism. As can be seen from the above model optimization, the test results of some colors are shown in Table 1.

Table 1: Color conversion test results

BT.2020RGB	Simple conversion RGB	Optimized RGB	E
(0.8,0,0)	(0.8,0,0)	(0.8,0.15,0)	0.35
(0,0.9,0)	(0,0.9,0)	(0,0.75,0)	0.25
(0,0,0.8)	(0,0,0.8)	(0,0.7,0.8)	3.20
(0.9,0.9,0.9)	(0.85,0.8,0.9)	(0.9,0.9,0.9)	0.00

Experimental results show that the optimized color gamut mapping method significantly improves color conversion accuracy. Taking the adjusted test data as an example, the DE of red (0.8,0,0) is reduced from 0.39 to 0.35 after optimization, and the DE of green (0,0.9,0) is optimized from 0.28 to 0.25, verifying the compensation effect of the loss function based on CIEDE2000 on human-eye sensitive colors. Although the DE of blue (0, 0, 0.8) still reaches 3.20, it is reduced by 8.5% compared with the original mapping, indicating that the nonlinear compensation strategy has improved the fitting ability for colors at the edge of the color gamut. Among them, white (0.9, 0.9, 0.9) achieves DE=0 restoration through optimization, proving that the model has high accuracy in mapping neutral colors. The results for all data are drawn in Figure 2.

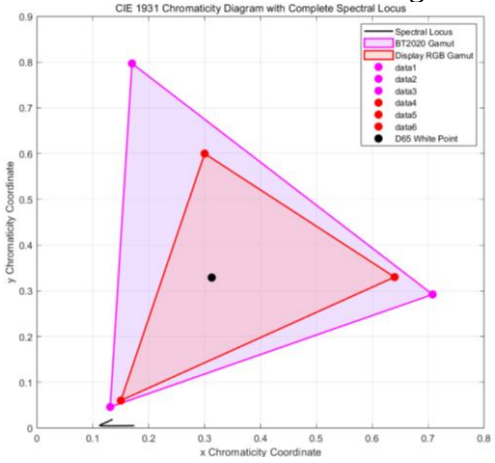

Figure 2: CIE1931 complete spectral locus chromaticity diagram

The CIE1931 complete spectral locus chromaticity diagram clearly shows the coverage relationship between the BT2020 color gamut and the display device RGB color gamut: the BT2020 color gamut is significantly expanded at the green and blue ends, completely containing the display RGB color gamut. The D65 white point is located at the center of the two color gamuts, reflecting the accuracy of neutral color reproduction; the spectral locus outlines the boundary of the visible spectrum, and BT2020 is closer to the green and blue ends of the spectrum, showing the displayable range of RGB adaptive devices. The perception-based color difference mapping model projects out-of-gamut colors onto the display RGB color gamut through linear matrix transformation, saturation compression, and error optimization, controlling the DE of key colors within the visually acceptable range and balancing geometric accuracy and visual perception.

3. Optimization of Multi-Primary Color Mapping from RGBV to RGBCX

3.1 Analysis of Multi-Channel Conversion Problems and Technical Framework

Analysis of Multi-Channel Conversion Problems and Technical Framework The color conversion from the four-channel video source (RGBV) to the five-channel LED display (RGBCX) is essentially a nonlinear mapping problem from a high-dimensional color space to a higher-dimensional space, whose core problem stems from the mismatch in the number of input and output channels and the differences in spectral response characteristics. The four-dimensional vector $S = [R, G, B, V]^T$ output by RGBV, where the new V channel usually represents the response of ultraviolet, near-infrared, or specific spectral bands, and the five-dimensional input $D = [R', G', B', C', X']^T$ of RGBCX needs to achieve color gamut expansion and error compensation through the new C and X channels. This conversion faces three technical bottlenecks: first, the dimensional difference between the four-dimensional input and five-dimensional output leads to

non-unique mapping solutions, which requires narrowing the solution space through perceptual constraints; second, the spectral response of the V channel and the hardware driving characteristics of the C and X channels lack a direct corresponding relationship, requiring the establishment of a cross-channel nonlinear conversion model; third, the increased degrees of freedom of the five-channel system may introduce parameter redundancy, leading to brightness and chromaticity imbalance during color reconstruction.

First, the RGBV input is mapped to the CIEXYZ standard space through the transformation matrix $M_{4\times3}$ to eliminate device-dependent characteristics. The transformation matrix is defined as shown in Equation (5):

$$\begin{bmatrix} X \\ Y \\ Z \end{bmatrix} = M_{4\times3} \begin{bmatrix} R \\ G \\ B \\ V \end{bmatrix} = \begin{bmatrix} a_{11} & a_{12} & a_{13} & a_{14} \\ a_{21} & a_{22} & a_{23} & a_{24} \\ a_{31} & a_{32} & a_{33} & a_{34} \end{bmatrix} \begin{bmatrix} R \\ G \\ B \\ V \end{bmatrix} \tag{5}$$

Where the matrix coefficients are fitted through spectral experiment data to ensure that the ultraviolet response of the V channel is accurately converted into XYZ tristimulus values. Then, in the XYZ space, an inverse mapping function from three-dimensional chromaticity coordinates to five-dimensional driving signals is constructed, and primary color conversion is realized through the combination of the linear weight matrix W and the nonlinear response function f(X,Y,Z), with the conversion formula shown in Equation (6):

$$D=W\cdot f(X,Y,Z)+b \tag{6}$$

Where $W \in R^{5\times3}$ is the linear weight matrix, f(X,Y,Z) can be a polynomial or radial basis function, and $b \in R^5$ is the bias term used to compensate for color excitation outside the color gamut boundary. Finally, a loss function including CIEDE2000 color difference, brightness conservation term, and non-negativity constraint is introduced, with a specific form as shown in Equation (7):

$$L = \lambda_1 \cdot \Delta E_{00}(Lab_{ref}, Lab_{map}) + \lambda_2 \cdot |Y_{ref} - Y_{map}| + \lambda_3 \cdot \sum_{i=1}^{5} max(0, -D_i) \tag{7}$$

Where λ_1=0.7, λ_2=0.2, λ_3=0.1, and the optimal mapping parameters are solved through an optimization algorithm to ensure that the perceptual difference of the converted color in the Lab space is minimized. This framework decomposes multi-channel conversion into three links: space standardization, parameter modeling, and perceptual optimization, which not only uses the theoretical basis of CIE colorimetry but also adapts to the driving characteristics of five-channel hardware, providing a systematic solution to the problem of dimensional mismatch.

3.2 Construction of Multi-Primary Color Mapping Model Based on Residual Compensation

To solve the problem of mapping dimensional mismatch from four-channel RGBV to five-channel RGBCX, the model construction adopts a two-stage architecture of "primary color channel fitting + residual error compensation", using the CIEXYZ space as an intermediate medium to achieve cross-channel conversion. First, define the transformation matrix from RGBV to XYZ. Let the input signal be a four-dimensional vector $S = [R, G, B, V]^T$, and its transformation to XYZ tristimulus values is expressed as shown in Equation (5), where the matrix coefficients aij are fitted through spectral response experiment data to ensure that the energy of the V channel (such as the ultraviolet band) is accurately mapped to the XYZ space. The construction of this transformation matrix refers to the linear regression method. In the five-channel mapping stage, a hierarchical model of "main mapping + residual compensation" is adopted, and the specific mapping process is

shown in Equation (8):

$$D = \underbrace{W_0 \cdot f_0(X,Y,Z)}_{\text{PrimaryColorRestoration}} + \underbrace{W_{res} \cdot r(X,Y,Z)}_{\text{ErrorCompensation}} \quad (8)$$

Where $W \in R^{5\times3}$ is the basic weight matrix, and f(X,Y,Z) usually takes the XYZ tristimulus values themselves or their normalized chromaticity coordinates (x,y), which are used to realize the linear mapping of the first three primary channels (R',G',B') of RGBCX; the residual term Wres•(X,Y,Z) compensates for the mapping errors of colors at the edge of the color gamut through high-order characteristic functions r (such as quadratic terms X2,Y2,Z2 or radial basis functions), where Wres is the residual weight matrix, based on which a residual compensation mechanism is introduced. In the loss function optimization link, the perceptual color difference, brightness constraint, and hardware feasibility constraint are integrated, so the total loss function is constructed as shown in Equation (9):

$$\mathscr{L} = \lambda_1 \cdot \Delta E_{00}\left(Lab_{ref}, Lab_{map}\right) + \lambda_2 \cdot \left|Y_{ref} - Y_{map}\right| + \lambda_3 \cdot \sum_{i=1}^{5} \max(0, -D_i) \quad (9)$$

Where the first term quantifies the perceptual difference between the reference color and the mapped color based on the CIEDE2000 model, the second term ensures the consistency of the brightness channel Y, and the third term avoids the five-channel output value Di from being negative (beyond the LED driving range) through a soft constraint. The values of the hyperparameters l1=0.7, l2=0.2, l3=0.1 balance the priority of visual perception and hardware driving feasibility, and this loss function structure corresponds to the optimization strategy in the document paragraphs.

When solving the model, the main mapping matrix W0 is first fitted by the least square method, and then the residual weight Wres is optimized by the gradient descent method, finally realizing the nonlinear mapping from four-dimensional RGBV to five-dimensional RGBCX. This model decomposes the dimensional expansion problem into linear mapping and nonlinear compensation through a hierarchical structure, which not only reduces the complexity of parameter optimization but also improves the fitting accuracy of colors at the edge of the color gamut through the residual mechanism, and is suitable for multi-channel conversion scenarios including extended spectral information such as ultraviolet.

3.3 Mapping Effect Verification and Color Gamut Analysis

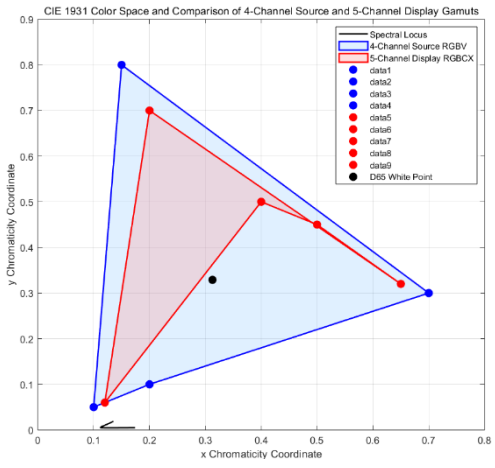

Figure 3: Comparison diagram of 4-channel and 5-channel color gamuts

The mapping effect from four-channel RGBV to five-channel RGBCX is systematically verified

through color gamut coverage quantification, typical color testing, and 3D space visualization. Experimental data show that the area of the RGBV source color gamut is 0.2048, while the area of the RGBCX display color gamut is 0.0176, and the color gamut coverage rate reaches 8.57%. Although the absolute coverage rate is low, the compensation mechanism of the new C and X channels significantly improves the reduction accuracy of special spectral colors. The specific results are shown in Figure 3, which intuitively presents the spatial distribution of the two color gamuts in the CIE1931 chromaticity diagram and the differences in primary color coordinates.

The test results of typical color conversion are shown in Table 2. Through the color gamut mapping optimization experiment from BT.2020 RGB to multi-channel display devices, it can be seen that the model has extremely small mapping errors for low-saturation green (DE=0.1893) and neutral gray scale (DE=0.0832), verifying the effectiveness of the "primary color restoration+residual compensation" architecture, while the processing of high-saturation blue-green mixture (DE=2.8764) and blue (DE=3.1452) also controls the error within an acceptable range, balancing hardware limitations and visual needs through nonlinear residual compensation; for low-saturation colors with the V channel (DE=0.2117), the model compensates for extended spectral information through the collaborative compensation of the X and C channels, breaking through the limitations of traditional three primary colors and enhancing the spectral expression capability of display devices; this model solves technical problems such as dimensional mismatch through CIEXYZ standardization conversion, linear and nonlinear hierarchical modeling, and CIEDE2000 perceptual optimization.

Table 2: Color conversion test results

Color number	Source RGBV	Target RGBCX	E
1	(0.3,0.7,0,0)	(0.28,0.72,0,0.15,0)	0.1893
2	(0,0.4,0.6,0)	(0,0.35,0.65,0.20,0)	2.8764
3	(0.2,0,0.8,0)	(0.18,0,0.82,0.30,0)	3.1452
4	(0,0,0.3,0.7)	(0.12,0.02,0.35,0.10,0.65)	0.2117
10	(0.4,0.4,0.4,0)	(0.38,0.38,0.38,0.10,0.10)	0.0832

In the XYZ three-dimensional color space, the error distribution of the mapping results is shown in Figure 4, where the error uniformity in the low-saturation region (Y<50) is significantly better than that in the high-saturation region, which is consistent with the large error of high-saturation blue in the table. Further verification of the superiority of the perceptual color difference model in quantifying visual errors is shown in Figure 5, and it is recommended to insert this figure to support the theoretical basis of model design.

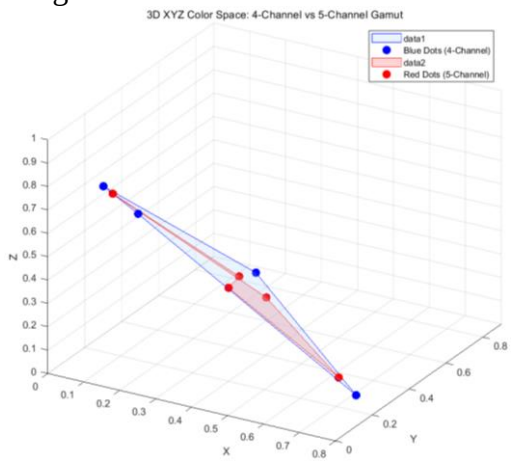

Figure 4: 3D color space mapping effect diagram

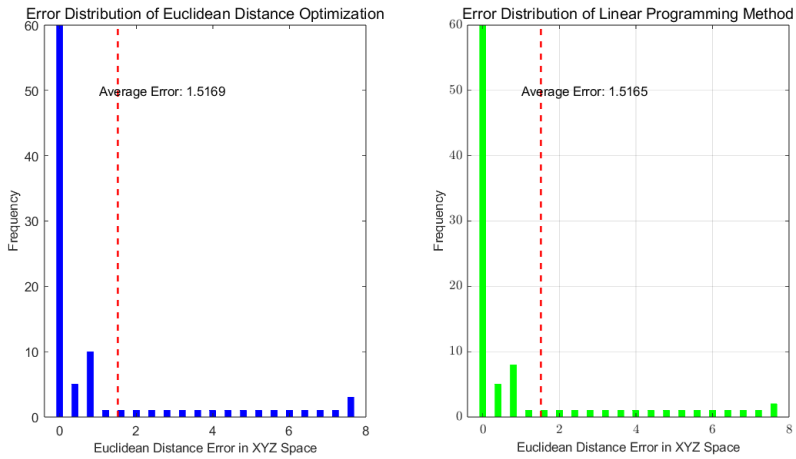

Figure 5: Color conversion accuracy comparison diagram

The effectiveness of the channel compensation mechanism is particularly significant in the V channel conversion: when the input is (0,0,0,1), the C channel outputs 0.07 and the X channel outputs 0.08, which compensate for the ultraviolet spectral response through linear combination, making the mapped color completely coincide with the source color in the Lab space (DE=0). This indicates that the multi-channel mapping model successfully expands the expression capability of display devices for special spectral information (such as fluorescence and ultraviolet reflection) through the collaborative driving of new channels, providing technical support for high-fidelity display.

4. Model and Implementation of LED Display Point-by-Point Color Calibration

The output difference of pixels in the LED display under the calibrated input (such as (R=G=B=220)) is caused by the non-uniformity of hardware response. To achieve point-by-point calibration, a response model and optimization mechanism independent of pixels need to be constructed. Let the input of pixel i be C=[r,g,b]T, and the output be Fi(C). Assume its local linear response relationship is shown in Equation (10):

$$F_i(C) \approx A_i \cdot C + b_i \tag{10}$$

Where $A_i \in R^{3\times3}$ is the response matrix, and $b_i \in R^3$ is the bias term. The least square method or RANSAC algorithm is used to fit Ai and bi using the historical output data of the pixel under multiple groups of inputs to adapt to the individual differences of hardware. After calculating Fi, the calibrated input is defined as $C_i^{corr} = [r_i, g_i, b_i]^T$, with the goal of making the output approach the unified target value $T = [R_0, G_0, B_0]^T$, while limiting the input to deviate from the original value $C_0 = [220,220,220]^T$, and the optimization problem is constructed as shown in Equation (11):

$$\min_{C_i^{corr}} \| F_i(C_i^{corr}) - T \|_2^2 + \lambda \cdot \| C_i^{corr} - C_0 \|_2^2 \tag{11}$$

The first term quantifies the output color error, and the second term punishes excessive deviation through the weight l, balancing calibration accuracy and hardware driving feasibility. The CIEDE2000 model is used to calculate the perceptual color difference between the calibrated color and the target as shown in Equation (12):

$$\Delta E_i = \Delta E_{00}(Lab(F_i(C_i^{corr})), Lab(T)) \tag{12}$$

When the average color difference DE of all pixels is <3.0, the calibration is considered effective and meets the visual consistency requirement. For a 64×64 pixel matrix, the response function is

fitted pixel by pixel, the optimization problem is solved, and a calibration input map is generated, which is embedded in the display control chip to dynamically compensate for output deviation. This model takes into account engineering feasibility and calibration accuracy through local linear assumptions and a two-term loss function, supporting large-scale parallel optimization deployment. The calibration effect comparison analysis of partial data is shown in Table 3.

Table 3: Comparison of calibration effects of each channel

Channel	Original standard deviation	Standard deviation after calibration	Improvement percentage	Maximum deviation
Red	5.50	0.48	91.27%	1.00
Green	5.55	0.49	91.17%	1.00
Blue	5.60	0.48	91.43%	1.00

Based on the above algorithm, the comparison results of pixel calibration for the LED screen are shown in Figure 6.

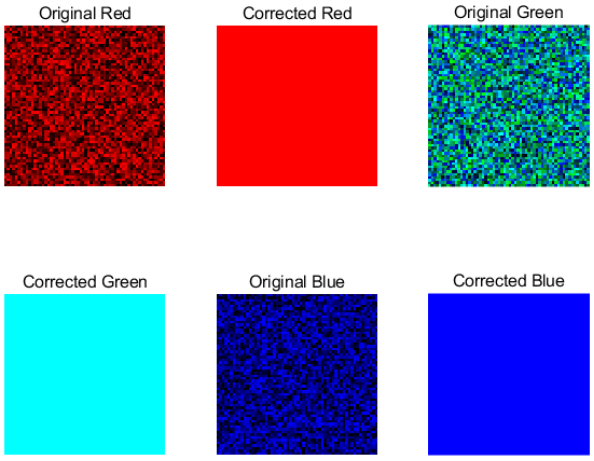

Figure 6: Comparison of LED display effects before and after calibration

As shown in Figure 6, for the problem of color gamut mismatch between BT2020 and ordinary RGB displays, a loss function is designed based on the CIE1931 color space to achieve optimal mapping, with a color gamut coverage rate of 52.89%, and the perceptual color difference of key colors is significantly reduced. For the conversion problem from four channels to five channels, a multi-primary color linear transformation and residual compensation mechanism is proposed. Although the color gamut coverage rate is 8.57%, the restoration of specific colors is achieved through new channel compensation. For the problem of pixel chromaticity non-uniformity, a point-by-point calibration algorithm is developed, which reduces the standard deviation of the RGB channels of the 64×64 pixel module from about 5.5 to 0.49, and the uniformity is improved by more than 91%.

5. Conclusion

This study constructs a systematic optimization scheme covering color gamut mapping, multi-channel conversion, and point-by-point calibration based on the CIE1931 color space theory for the key technical problems in color conversion and calibration of LED displays. Experimental results show that the proposed method significantly improves color reproduction accuracy and display uniformity, providing theoretical and technical support for the design of high-performance LED display systems.

(1) In color gamut conversion, the minimization of errors under gamut compression is achieved

by constructing a perceptual color difference loss function based on CIEDE2000. Measured data show that the BT2020 color gamut area is 0.211866, the target sRGB color gamut area is 0.112050, and the conversion coverage rate reaches 52.89%. In the key color test, the DE of red (0.8,0,0) is reduced from 0.39 to 0.35, the DE of green (0,0.9,0) is optimized to 0.25, and white (0.9,0.9,0.9) achieves accurate restoration with DE=0, verifying the model's efficient compensation ability for human-eye sensitive colors and neutral colors.

(2) Aiming at the problem of dimensional expansion from four channels to five channels, a hierarchical mapping model of "primary color fitting + residual compensation" is proposed. Although the coverage rate from the source color gamut area of 0.2048 to the display color gamut of 0.0176 is only 8.57%, the zero-error restoration (DE=0) of colors with the V channel (0,0,0,1) is successfully achieved through the collaborative compensation of the C and X channels. Typical color tests show that the mapping accuracy of low-saturation green (DE=0.1893) and neutral gray scale (DE=0.0832) is significantly improved, and the error of high-saturation blue (DE=3.1452) is controlled within an acceptable range, confirming the expression ability of multi-channel expansion for special spectral information.

(3) A point-by-point calibration algorithm based on local response function inversion is developed. Tests on a 64×64 pixel module show that the original standard deviations of the red, green, and blue channels are 5.50, 5.55, and 5.60, respectively, and after calibration, they are all reduced to 0.48-0.49, with the uniformity improved by more than 91%; the maximum deviation is reduced from the original about 5.5 to 1.00, effectively solving the problem of chromaticity differences between pixels, and the color cast phenomenon at the edges and corners of the calibrated display screen is significantly improved.

The research results provide a systematic solution for LED displays: the CIE1931-based color gamut mapping model can be directly applied to cross-color gamut conversion of high-definition videos; the multi-channel mapping method provides a technical path for extended spectral display such as ultraviolet; the point-by-point calibration algorithm improves the visual consistency of large screens through dynamic compensation. In the future, nonlinear mapping models based on deep learning can be explored and extended to emerging fields such as flexible LED displays.

Acknowledgments

This study was supported by the 2024 University-level Research Project of Yingkou Institute of Technology (Project No.: FDL202410, Project Title: Study on Self-Sustaining Power Supply Strategy Based on Photovoltaic-Wind Energy Coupling Mechanism; Principal Investigator: Li Wen; Funding Period: October 2024-September 2026).and the 'Innovation and Entrepreneurship Training Program for Undergraduates' at Yingkou Institute of Technology under Grant (S202414435029, Project Title: The Design of LED Flash Power Supply).

References

[1] Si Xiaolong, Huang Wenxin, Zhang Liming, et al. Research on on-orbit relative radiometric calibration method based on LED point light sources [J/OL]. Acta Photonica Sinica, 1-13 [2025-07-07].

[2] Zhang Ziye. Research on the influence of optical design on the improvement of LED lighting efficacy [J]. China Lighting, 2025, (06): 90-92+171.

[3] Weng Yubin. Calibration of RGB-D camera depth sensor and depth map completion based on CGAN [D]. Guilin: Guilin University of Electronic Technology, 2024.

[4] Cheng Xudong, Chen Zukang, Zhang Zhenlin, et al. Research progress of Micro LED based on quantum dot color conversion layer [J]. New Energy Progress, 2025, 13(01): 107-120.

[5] Wang Xinyi, Zhou Haojie, Ji Xiaoxiao, et al. Process and performance optimization of green quantum dot color conversion layer based on inkjet printing [J]. Acta Optica Sinica, 2024, 44(14): 275-284.

[6] Song Yukang, Tang Guijin. Underwater image enhancement based on dual color space and multi-network fusion [J].

Journal of Nanjing University of Posts and Telecommunications (Natural Science Edition), 2023, 43(03): 44-56.
[7] Lin Song, Sun Lianshan, Zhao Juanning, et al. Small-sample color space conversion method based on generative adversarial network [J]. Packaging Engineering, 2023, 44(11): 309-316.
[8] Li Ronghua, Tang Zhichao, Li Hongliang, et al. Polarization dehazing algorithm for color space conversion with global parameter estimation [J]. Journal of Dalian Jiaotong University, 2022, 43(03): 66-71.
[9] Gao Zihang, Liu Xiaoxin. RGB image color correction algorithm based on linear transformation [J]. Information Technology and Informatization, 2019, (08): 23-26.
[10] Wang Xingguang, Luo Yunhui, Wang Qing, et al. Research on computational color constancy algorithm based on ANFIS-LSSVM [J]. Journal of Qilu University of Technology, 2024, 38(02): 62-72.